arXiv:1404.1200v2 [hep-ph] 22 Apr 2014

OCHA-PP-320
April 2014

Production and decay of radion in Randall-Sundrum model at a photon collider

Gi-Chol Cho[a] and Yoshiko Ohno[b]

[a] *Department of Physics, Ochanomizu University, Tokyo 112-8610, Japan*
[b] *Graduate School of Humanities and Sciences, Ochanomizu University, Tokyo 112-8610, Japan*

Abstract

A warped extra dimension model predicts an extra scalar particle beyond the Standard Model which is called a radion. Although interactions of the radion are similar to those of the Higgs boson in the Standard Model, a relatively light radion ($\lesssim 100$ GeV) is not severely constrained from the Higgs search experiments at the LHC. In this paper we study discovery potential of the radion at a photon collider as an option of ILC. Owing to the trace anomaly of the energy-momentum tensor, both a production of radion in $\gamma\gamma$ collision and its decay to gluon pair are enhanced sizably. We find that the photon collider has a sensitivity for discovering the radion in low-mass region up to $\Lambda_\phi \sim 3$ TeV, where Λ_ϕ is a scale parameter which suppresses the interactions of radion to the Standard Model particles.

1 Introduction

A warped extra dimension model proposed by Randall and Sundrum (RS) is one of the attractive candidates to solve the gauge hierarchy problem in the Standard Model (SM) naturally [1]. The model is given in the five-dimensional space-time where one warped extra dimension is compactified on the orbifold S^1/Z_2. The space-time metric is given by

$$ds^2 = e^{-2ky}\eta_{\mu\nu}dx^\mu dx^\nu - dy^2 \ , \tag{1}$$

where $x^\mu(\mu = 0, 1, 2, 3)$, y and k denote the coordinate of four-dimensional space-time, that of a fifth dimension, and the AdS_5 curvature, respectively. The Minkowski metric is $\eta_{\mu\nu} = \mathrm{diag}(+1, -1, -1, -1)$ and e^{-2ky} is called a warp factor. Two 3-branes are located at $y = 0$ and πr_c. They are called the UV brane ($y = 0$) and the IR brane ($y = \pi r_c$). In the original RS model all the SM fields are confined on the IR brane and only graviton is allowed to propagate into the bulk. There are some variants of the RS model where some of SM fields propagate in the extra dimension [2, 3].

With this setup, the four dimensional Planck mass M_{pl} is expressed by a fundamental parameter M in the five dimensional Einstein-Hilbert action as

$$M_{\mathrm{pl}}^2 = \frac{M^3}{k}(1 - e^{-2ky}), \tag{2}$$

As a result, an effective mass parameter in the IR brane is given as $M_{\mathrm{pl}}e^{-k\pi r_c}$, and the gauge hierarchy problem could be solved naturally when the distance between UV and IR branes are stabilized by $kr_c \sim 12$. Goldberger and Wise have proposed an attractive mechanism to stabilize the distance between two branes introducing a bulk scalar field which has scalar potentials on both branes [4]. Minimizing the scalar potentials on the branes, the distance between two branes takes appropriate value ($kr_c \sim 12$) without fine-tuning of the parameters in the scalar potentials. In four dimensional effective theory of the original RS model, there are two new particles beyond the Standard Model. One is a spin-2 graviton (and its Kaluza-Klein excitations) and the other is a scalar-field radion ϕ which is a metric fluctuation along the extra dimension. The radion acquires the mass of the order of the electroweak scale due to the Goldberger-Wise mechanism and it could be a lightest extra particle in the RS model [4, 5]. The radion, therefore, is expected to be the first signature of warped extra dimension models in direct search experiments such as the LHC. Phenomenology of the radion can be characterized by two parameters, a radion mass m_ϕ and a scale parameter Λ_ϕ.

The search experiments of the Higgs boson at the LHC give stringent constraints on the parameters of the radion. As will be shown later, the radion couples to the trace part of the energy-momentum tensor of the SM. Thus it is known that the interactions of the radion to the SM particles such as electroweak gauge bosons ($W^\pm, Z$) and fermions are similar to those of the Higgs boson, except for the scale parameters in the couplings. On the

other hand, the interactions of radion to photons and gluons have additional source from the trace anomaly of the energy-momentum tensor in addition to the 1-loop contributions from W boson and/or fermions as in the SM. Furthermore, there could be a mixing between the radion and the SM Higgs boson through the scalar-curvature mixing term in the four-dimensional effective action [6, 7]. According to these characteristic features of the radion interactions, there have been studied the phenomenological aspects of the radion in various colliders [8, 9, 10, 11, 12, 13, 14].

It has been reported that the Higgs boson mass m_h is 126.0 ± 0.4(stat.)± 0.4(syst.) GeV at ATLAS [15] and 125.3 ± 0.4(stat.)± 0.5(syst.) GeV at CMS [16], respectively, and there is no signature of any other scalar particles up to 600 GeV from the ZZ mode. Thus one can apply the results of the Higgs search experiments at the LHC to constrain the mass and couplings of the radion. Recently, the bounds on the parameters m_ϕ and Λ_ϕ were studied in light of the Higgs boson discovery at the LHC using $pp \to h \to \gamma\gamma, ZZ, W^+W^-$ [9, 17]. It was found that constraint on the parameter Λ_ϕ for the high-mass region of the radion ($m_\phi \lesssim 1$ TeV) from the ZZ mode is much severe than results in the previous studies [18, 19]. It is, however, pointed out that the radion in low-mass region ($m_\phi \sim 100$ GeV) is not constrained at the LHC, i.e., the Higgs search in the $\gamma\gamma$ channel at the LHC is less sensitive to a relatively light radion, since the $\phi \to gg$ mode dominates over the other decay modes in this region which suppresses the branching ratio of $\phi \to \gamma\gamma$. Then it is worth examining possibilities to search for the radion in the low-mass region in collider experiments.

In this paper, we study production and decay of the radion at a photon collider which has been proposed as an option of an e^+e^- linear collider such as the ILC [20]. It has been studied that the photon collider has an advantage to distinguish the radion produced in the $\gamma\gamma$ collision from the SM Higgs boson production [21, 22, 23] supposing the SM Higgs boson is relatively heavy. The production of radion in the light-by-light scattering at the LHC has been discussed in ref. [24]. We show that the decay of radion in low-mass region into gluon pair is a promissing channel for its discovery at photon collider.

This paper is organized as follows. In Sec. 2, we briefly review the interactions of radion to SM fields with emphasis on the difference from those of the SM Higgs boson. Production and decay of the radion at the photon collider are discussed in Sec. 3. We show our numerical results in Sec. 4 where a discovery potential of the radion at the photon collider is discussed quantitatively. Sec. 5 is devoted to summary and discussion.

2 Interactions

The radion field represents a fluctuation of the distance between the UV and IR branes. Taking account of a fluctuation along the fifth dimension, the metric is written as [7]

$$ds^2 = e^{-2(ky+F(x,y))}\eta_{\mu\nu}dx^\mu dx^\nu - (1+2F(x,y))^2 dy^2, \tag{3}$$

where $F(x,y)$ is a scalar perturbation. A canonically normalized radion field ϕ is given by [7]

$$F(x,y) = \frac{\phi}{\Lambda_\phi} e^{2k(y-\pi r_c)}, \tag{4}$$

where the scale parameter Λ_ϕ is $\mathcal{O}(\mathrm{TeV})$ [7, 25].

The radion couples to the trace part of the energy-momentum tensor of the SM. Then, the interaction Lagrangian of the radion is given by

$$\mathcal{L}_{\rm int} = \frac{\phi}{\Lambda_\phi} T^\mu_{\ \mu}, \tag{5}$$

where $T^\mu_{\ \mu}$ is the trace of energy-momentum tensor of the SM which is given as

$$\begin{aligned} T^\mu_{\ \mu} &= -2m_W^2 W_\mu^+ W^{-\mu} - m_Z^2 Z_\mu Z^\mu + \sum_f m_f \bar{f} f + (2m_h^2 h^2 - \partial_\mu h \partial^\mu h) \\ &+ \frac{\beta_{\rm QED}}{2e} F_{\mu\nu} F^{\mu\nu} + \frac{\beta_{\rm QCD}}{2g_s} G^a_{\mu\nu} G^{a\mu\nu} + \cdots, \end{aligned} \tag{6}$$

$$\beta_{\rm QED} = \left(\frac{1}{16\pi}\right)^2 \left(\frac{19}{6} g_2^3 - \frac{41}{6} g_Y^3\right), \tag{7}$$

$$\beta_{\rm QCD} = \left(\frac{1}{16\pi}\right)^2 \left(11 - \frac{2}{3} n_f\right) g_s^3, \tag{8}$$

where the first line in r.h.s. of (6) is obtained from the energy-momentum tensor of the SM. Two terms in the second line of (6) come from the trace anomaly for photons ($F_{\mu\nu}$) and gluons ($G^a_{\mu\nu}, a = 1, \cdots, 8$), respectively, and the ellipsis denote the higher-order terms. The number of active quark-flavors is denoted by n_f[1]. We can see from (6) that, except for the trace anomaly terms, the interactions of the radion to the SM fields are very similar to those of the SM Higgs boson. The interactions of the radion are, however, suppressed by the scale parameter $\Lambda_\phi \sim O(\mathrm{TeV})$ which corresponds to the Higgs vacuum expectation value, $v = 246\mathrm{GeV}$, in the interactions of the SM Higgs boson to other SM fields.

It is worth mentioning that, in general, the radion and the Higgs boson can mix after the electroweak symmetry breaking through the scalar-curvature term in the four-dimensional effective action [6, 7]. In our following study, however, we do not consider the mixing between the radion and the Higgs boson, since the current experimental results of the Higgs searches at the LHC tell us that the measured branching ratios of the Higgs boson are consistent with those in the SM [15, 16], so that we can neglect the radion-Higgs mixing in a good approximation.

3 Production and decay of radion at a photon collider

The production cross section of the radion in the $\gamma\gamma$ collision, and the branching fractions are obtained from the interaction Lagrangian in eq. (5). In the photon collider, the high

[1] We take $n_f = 6$ in our analysis.

energy photons are obtained from electron beams through the inverse Compton scattering. The convoluted production cross section with energy distribution of photon beams is given by [22, 23, 26, 27]

$$\sigma(s) = \int_{m_\phi/\sqrt{s}}^{x_{max}} dz \left[2z \int_{z^2/x_{max}}^{x_{max}} \frac{dx}{x}\, f_\gamma(x) f_\gamma\Big(\frac{z^2}{x}\Big) \right] \times \hat{\sigma}_{\gamma\gamma\to\phi}(\hat{s}), \tag{9}$$

where $\sqrt{s}$ and $\sqrt{\hat{s}}$ represent the center-of-mass energy of electron pair and $\gamma\gamma$ systems, respectively. A momentum fraction of a photon against the electron momentum is denoted by x, and z is defined by $z^2 = \hat{s}/s$. The production cross section of the radion in the $\gamma\gamma$ annihilation $\hat{\sigma}_{\gamma\gamma\to\phi}(\hat{s})$ can be expressed using the decay rate of $\phi \to \gamma\gamma$ as

$$\begin{aligned} \hat{\sigma}_{\gamma\gamma\to\phi}(\hat{s}) &= \frac{4\pi^2}{\hat{s}}\, \delta(\sqrt{\hat{s}} - m_\phi)\, \Gamma(\phi \to \gamma\gamma) \\ &= \frac{4\pi^2}{z s \sqrt{s}}\, \delta\Big(z - \frac{m_\phi}{\sqrt{s}}\Big)\, \Gamma(\phi \to \gamma\gamma)\ . \end{aligned} \tag{10}$$

A function $f_\gamma(x)$ in (9) is the unpolarized photon flux from the laser back-scattering

$$f_\gamma(x) = \frac{1}{D(\xi)} \left(1 - x + \frac{1}{1-x} - \frac{4x}{\xi(1-x)} + \frac{4x^2}{\xi^2 (1-x)^2} \right), \tag{11}$$

where

$$D(\xi) = \left(1 - \frac{4}{\xi} - \frac{8}{\xi^2} \right) \ln(1+\xi) + \frac{1}{2} + \frac{8}{\xi} - \frac{1}{2(1+\xi)^2}\ . \tag{12}$$

A parameter ξ is chosen to be $\xi = 4.8$, then $D(\xi) = 1.8$ and $x_{max} = 0.83$ [26].

In Fig. 1, the production cross section (9) is given as a function of m_ϕ for $\Lambda_\phi = 1$ TeV (a) and 3 TeV (b), respectively. Three curves in black, red and blue in each figure correspond to $\sqrt{s} = 250$ GeV, 500 GeV and 1 TeV, respectively. For each $\sqrt{s}$, the cross section is enhanced around $m_\phi = 150 - 200$ GeV. Note that the threshold energy of electron collision for the radion production is somewhat smaller than m_ϕ since the radion is produced via collision of back-scattered photons. For example, in Fig. 1 (a), the production cross section is larger than 1 fb for $m_\phi \lesssim 400$ GeV ($\sqrt{s} = 500$ GeV) and $m_\phi \lesssim 820$ GeV ($\sqrt{s} = 1$ TeV).

The decay widths of the radion to the SM particles are easily calculated from eq. (5):

$$\Gamma(\phi \to gg) = \frac{\alpha_s^2 m_\phi^3}{32\pi^3 \Lambda_\phi^2} \left| b_{\rm QCD} + x_t \left\{1 + (1-x_t) f(x_t)\right\}\right|^2 , \tag{13}$$

$$\Gamma(\phi \to \gamma\gamma) = \frac{\alpha_{\rm em}^2 m_\phi^3}{256\pi^3 \Lambda_\phi^2} \Bigg| b_2 + b_Y - \left\{2 + 3x_W + 3x_W(2-x_W) f(x_W)\right\} + \frac{8}{3} x_t \left\{1 + (1-x_t) f(x_t)\right\} \Bigg|^2 , \tag{14}$$

$$\Gamma(\phi \to Z\gamma) = \frac{\alpha_{\rm em}^2 m_\phi^3}{128\pi^3 s_{\rm w}^2 \Lambda_\phi^2} \left(1 - \frac{m_Z^2}{m_\phi^2}\right)^3 \times \left| \sum_f N_f \frac{Q_f}{c_{\rm W}} \hat{v}_f \; A_{1/2}^\phi(x_f, \lambda_f) + A_1^\phi(x_W, \lambda_W) \right|^2 , \tag{15}$$

$$\Gamma(\phi \to f\bar{f}) = \frac{N_c m_f^2 m_\phi}{8\pi \Lambda_\phi^2} (1 - x_f)^{3/2}, \tag{16}$$

$$\Gamma(\phi \to W^+W^-) = \frac{m_\phi^3}{16\pi \Lambda_\phi^2} \sqrt{1 - x_W} \Big(1 - x_W + \frac{3}{4} x_W^2\Big), \tag{17}$$

$$\Gamma(\phi \to ZZ) = \frac{m_\phi^3}{32\pi \Lambda_\phi^2} \sqrt{1 - x_Z} \Big(1 - x_Z + \frac{3}{4} x_Z^2\Big), \tag{18}$$

$$\Gamma(\phi \to hh) = \frac{m_\phi^3}{32\pi \Lambda_\phi^2} \sqrt{1 - x_h} \Big(1 + \frac{1}{2} x_h\Big)^2, \tag{19}$$

where $(b_{\rm QCD}, b_2, b_Y) = (7, 19/6, -41/6)$. A symbol f denotes all quarks and leptons. Two variables x_i and λ_i are defined as $x_i = 4m_i^2/m_\phi^2$ $(i = t, f, W, Z, h)$ and $\lambda_i = 4m_i^2/m_Z^2$ $(i = f, W)$. The gauge couplings for QCD and QED are given by α_s and $\alpha_{\rm em}$, respectively. The factor N_f is the number of active quark-flavors in the 1-loop diagrams and N_c is 3 for quarks and 1 for leptons. Q_f and $\hat{v}_f$ denote the electric charge of the fermion and the reduced vector coupling in the $Zf\bar{f}$ interactions $\hat{v}_f = 2I_f^3 - 4Q_f s_W^2$, where I_f^3 denotes the weak isospin and $s_W^2 \equiv \sin^2\theta_W$, $c_W^2 = 1 - s_W^2$. The form factors $A_{1/2}^\phi(x,\lambda)$ and $A_1^\phi(x,\lambda)$ are given by

$$A_{1/2}^\phi(x,\lambda) = I_1(x,\lambda) - I_2(x,\lambda) \; , \tag{20}$$

$$A_1^\phi(x,\lambda) = c_W \left\{ 4\left(3 - \frac{s_W^2}{c_W^2}\right) I_2(x,\lambda) + \left[\left(1 + \frac{2}{x}\right)\frac{s_W^2}{c_W^2} - \left(5 + \frac{2}{x}\right)\right] I_1(x,\lambda) \right\} .$$

The functions $I_1(x,\lambda)$ and $I_2(x,\lambda)$ are

$$I_1(x,\lambda) = \frac{x\lambda}{2(x-\lambda)} + \frac{x^2\lambda^2}{2(x-\lambda)^2}[f(x^{-1}) - f(\lambda^{-1})] + \frac{x^2\lambda}{(x-\lambda)^2}[g(x^{-1}) - g(\lambda^{-1})] \; ,$$

$$I_2(x,\lambda) = -\frac{x\lambda}{2(x-\lambda)}[f(x^{-1}) - f(\lambda^{-1})] \; , \tag{21}$$

where the loop functions $f(x)$ and $g(x)$ in (13), (14) and (21) are given by [23, 28]

$$f(x) = \begin{cases} \left\{ \sin^{-1}\left(\frac{1}{\sqrt{x}}\right) \right\}^2 & , \quad x \geq 1 \\ -\frac{1}{4}\left(\log \frac{1+\sqrt{1-x}}{1-\sqrt{1-x}} - i\pi \right)^2 & , \quad x < 1 \end{cases} , \tag{22}$$

$$g(x) = \begin{cases} \sqrt{x^{-1}-1}\sin^{-1}\sqrt{x} & , \quad x \leq 1 \\ \frac{\sqrt{1-x^{-1}}}{2}\left(\log \frac{1+\sqrt{1-x^{-1}}}{1-\sqrt{1-x^{-1}}} - i\pi \right) & , \quad x > 1 \end{cases} . \tag{23}$$

The branching ratio of the radion for all possible decay modes as a function of m_ϕ is shown in Fig. 2. The mass of Higgs boson is fixed at $m_h = 125$ GeV in the figure. We can see from Fig. 2 that the dominant decay mode is $\phi \to gg$ for $m_\phi \lesssim 150$ GeV while it is altered by $\phi \to W^+W^-$ for $2m_W \lesssim m_\phi$. The decay into ZZ or hh are subdominant for $2m_i \lesssim m_\phi$ $(i = Z, h)$.

We note here that the dominant decay mode of the radion at low-mass region is $\phi \to gg$ while that of the SM Higgs boson is $h \to b\bar{b}$. This is because that the interaction in the former is enhanced by the trace anomaly of the energy-momentum tensor as mentioned in a previous section.

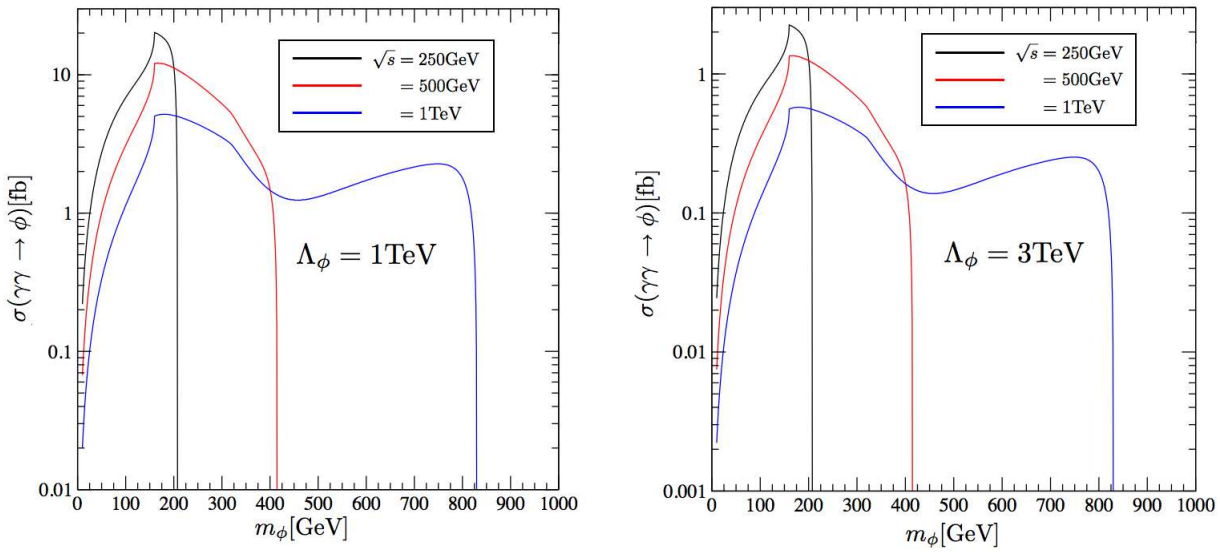

(a) (b)

Figure 1: The production cross sections of the radion at a photon collider given in Eq. (9) as a function of radion mass m_ϕ with $\Lambda_\phi = 1$TeV (a) and $\Lambda_\phi = 3$TeV (b). The curves correspond to the electron beam energy $\sqrt{s} = 250$ GeV (black), 500 GeV (red) and 1 TeV (blue).

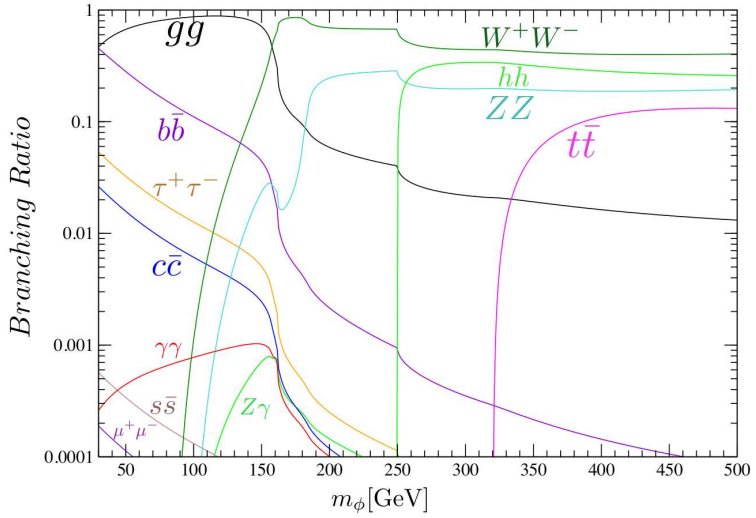

Figure 2: The branching ratio of radion for each decay modes as a function of m_ϕ. The mass of the SM Higgs boson is fixed at $m_h = 125$ GeV.

4 Numerical analysis

In this section, we discuss a discovery potential of the radion in low-mass region ($m_\phi \lesssim 150$ GeV) at the photon collider focusing on the signal process $\gamma\gamma \to \phi \to gg$, which is expected to be enhanced by the trace anomaly in both production and decay processes. At the photon collider, the leading background is $\gamma\gamma \to h \to gg$. Then we survey the model parameter space (m_ϕ, Λ_ϕ) by requiring a significance $S/\sqrt{B} > 5$ by defining both S and B as

$$S = \int \mathcal{L}_{\mathit{eff}}\, dt \times \sigma(ee \to \phi) \times \mathrm{Br}(\phi \to gg), \tag{24}$$

$$B = \int \mathcal{L}_{\mathit{eff}}\, dt \times \sigma(ee \to h) \times \mathrm{Br}(h \to gg). \tag{25}$$

The production cross section $\sigma(e^+e^- \to \phi)$ is identical to that in (9), and $\sigma(e^+e^- \to h)$ is obtained replacing $\hat{\sigma}_{\gamma\gamma\to\phi}(\hat{s})$ in (10) by $\hat{\sigma}_{\gamma\gamma\to h}(\hat{s})$. The effective photon luminosity $\int \mathcal{L}_{\mathit{eff}}\, dt$ is assumed to be 1/3 of the electron luminosity following the TESLA technical design report [29]. In our numerical analysis, we fix the Higgs boson mass m_h at 125 GeV for simplicity.

Although the dominant decay channel is $\phi \to gg$ for $m_\phi \lesssim 150$ GeV, it is altered by $\phi \to VV$ $(V = W^\pm, Z)$ for $2m_W \lesssim m_\phi$. It is very hard to study the radion production and decay using the W^+W^- channel since $\gamma\gamma \to W^+W^-$ occurs at the tree level in the SM and it overwhelms the signal process. Thus we use the ZZ channel instead of W^+W^-, and estimate $S/\sqrt{B}$ assuming that B is dominated by the $h \to ZZ$ channel as a reference in the high-mass region.

In Fig. 3, we show the signal region on m_ϕ-Λ_ϕ plane where $S/\sqrt{B} > 5$ is expected for various $\sqrt{s}$ and the effective integrated luminosity of back-scattered photon $\int \mathcal{L}_{\mathit{eff}} dt$. The

expected beam luminosity of ILC is $(0.75, 1.8, 3.6) \times 10^{34}\text{cm}^{-2}\text{s}^{-1}$, for $\sqrt{s} = 250$ GeV, 500 GeV, 1 TeV [20, 30]. Therefore we used $\int \mathcal{L}_{\mathit{eff}} dt = 80$ fb^{-1}, 160 fb^{-1} and 330 fb^{-1} in Fig. 3 (a), (b) and (c). In the figure, black and red regions correspond to $S/\sqrt{B} > 5$ for the $\phi \to gg$ and $\phi \to ZZ$ channels, respectively. It is also shown the excluded region on (m_ϕ, Λ_ϕ) plane [17] taking account of the Higgs search experiments at the LHC [32, 33, 34]. Turquoise, purple and magenta regions are excluded from the $pp \to h \to ZZ$, $pp \to h \to W^+W^-$ and $pp \to h \to \gamma\gamma$ in the Higgs searches at the LHC.

From the figure, we find that the significance $S/\sqrt{B}$ at least 5 is achieved in both the gg and ZZ channels. When $m_\phi \lesssim 150$ GeV, $S/\sqrt{B} > 5$ is possible for $\Lambda_\phi \lesssim 3$ TeV in (a), (b) and (c). On the other hand, the ZZ mode is available only for 180 GeV $\lesssim m_\phi$. In the ZZ mode, although there are sizable regions with $S/\sqrt{B} > 5$ in (b) and (c), these regions are entirely disfavored from the Higgs search experiments at the LHC. We, therefore, expect that the photon collider has a good chance for discovery of the radion with $m_\phi \lesssim 150$ GeV but it has no sensitivity to search for the radion if the mass is larger than 180 GeV.

We have so far focused on the gluon final state in the radion decay. In the experiment, the two gluons in the final state are observed as two jets which also contain quarks. Since $\gamma\gamma \to q\bar{q}$ occurs at the tree level, it is very crucial to separate the gluon final states from $\gamma\gamma \to jj$. The detectors at ILC are aiming to achieve a high efficiency of tagging the b and c quark flavors [30, 31]. Subtracting b and c jets from the data, and requiring appropriate kinematical cuts, it is expected to obtain two gluons in dijet data with a certain efficiency. A more quantitative estimation on the background (including $\gamma\gamma \to q\bar{q}$) processes is necessary based on the Monte Carlo simulation, which will be done elsewhere [35].

5 Summary

We have studied production and decay of the radion in the RS model at a photon collider as an option of e^+e^- linear collider (ILC). Owing to the trace anomaly of the energy-momentum tensor, the interactions of the radion to photons and gluons are much enhanced. Focusing on the gluon final states in the radion decay, which is a dominant decay mode in the low-mass region of the radion, we investigated the model parameter space where the significance $S/\sqrt{B} > 5$, and found that it could be achieved for $\Lambda_\phi \lesssim 3$ TeV and $m_\phi \lesssim 150$ GeV, without conflicting the constraints from the LHC experiments. To be more realistic, it is necessary to estimate both signal and background (including $\gamma\gamma \to q\bar{q}$) processes using the Monte Carlo simulation. The photon collider could be a good stage to look for the radion in the low-mass region which LHC experiment does not cover.

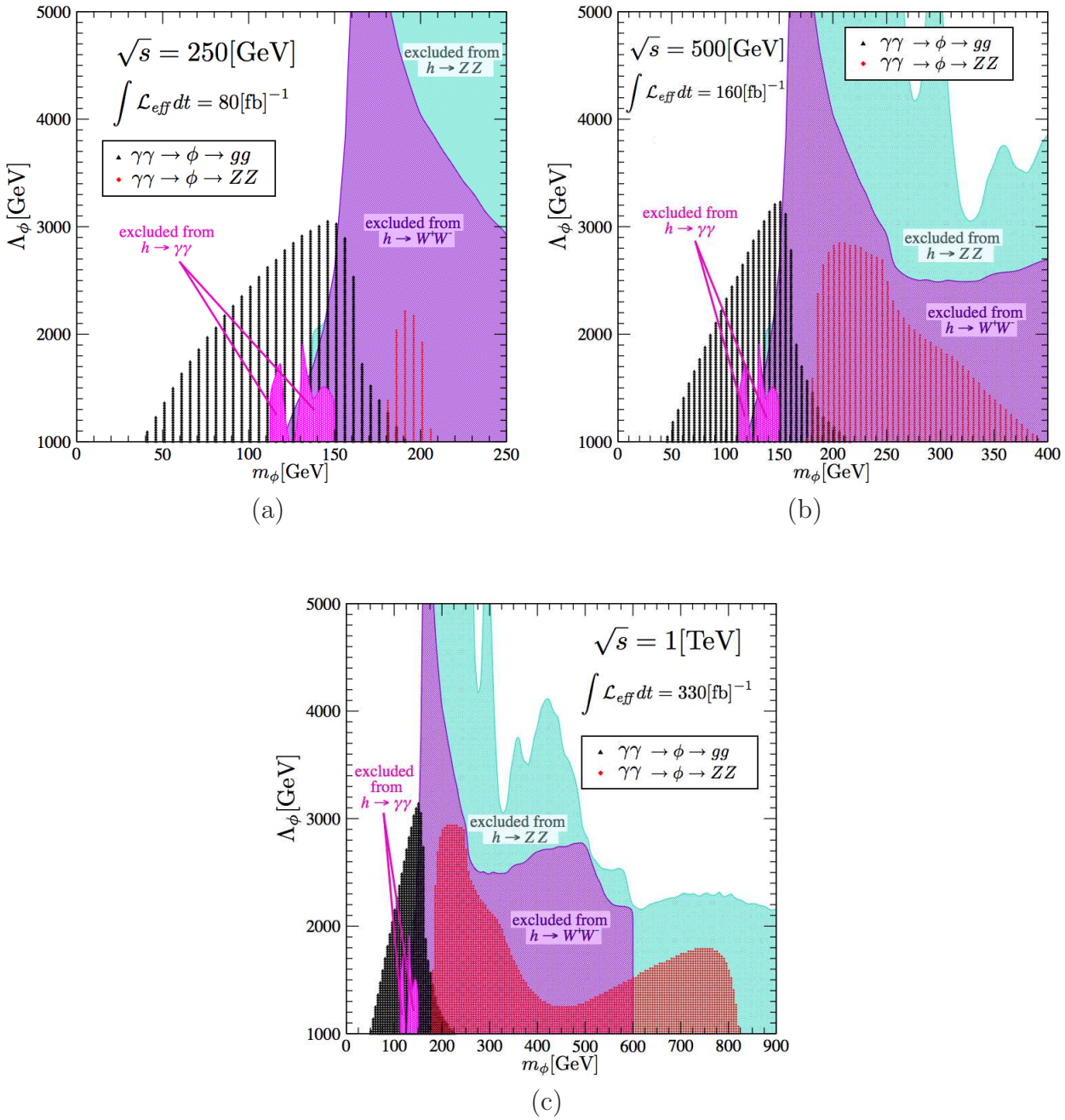

Figure 3: Signal regions on $(m_\phi,\ \Lambda_\phi)$ plane for various beam energy of electron $\sqrt{s} =$ 250 GeV (a), 500 GeV (b) and 1 TeV (c). The excluded regions from the recent results from the LHC are also shown [17]. Black and red regions denote parameter regions where signal significance $S/\sqrt{B} > 5$ for $\gamma\gamma \to \phi \to gg$ and $\gamma\gamma \to \phi \to ZZ$ processes, respectively. Region in turquoise, purple and magenta show the 95% CL excluded region from $pp \to h \to ZZ$, $pp \to h \to W^+W^-$ and $pp \to h \to \gamma\gamma$ processes at the LHC.

Acknowledgements

The work of G.C.C is supported in part by Grants-in-Aid for Scientific Research from the Ministry of Education, Culture, Sports, Science and Technology (No.24104502) and from the Japan Society for the Promotion of Science (No.21244036).

References

[1] L. Randall and R. Sundrum, "A Large mass hierarchy from a small extra dimension," Phys. Rev. Lett. **83**, 3370 (1999) [hep-ph/9905221].

[2] H. Davoudiasl, J. L. Hewett and T. G. Rizzo, "Bulk gauge fields in the Randall-Sundrum model," Phys. Lett. B **473**, 43 (2000) [hep-ph/9911262].

[3] H. Davoudiasl, J. L. Hewett and T. G. Rizzo, "Experimental probes of localized gravity: On and off the wall," Phys. Rev. D **63**, 075004 (2001) [hep-ph/0006041].

[4] W. D. Goldberger and M. B. Wise, "Modulus stabilization with bulk fields," Phys. Rev. Lett. **83**, 4922 (1999) [hep-ph/9907447].

[5] G. D. Kribs, "TASI 2004 lectures on the phenomenology of extra dimensions," hep-ph/0605325.

[6] G. F. Giudice, R. Rattazzi and J. D. Wells, "Graviscalars from higher dimensional metrics and curvature Higgs mixing," Nucl. Phys. B **595**, 250 (2001) [hep-ph/0002178].

[7] C. Csaki, M. L. Graesser and G. D. Kribs, Phys. Rev. D **63**, 065002 (2001) [hep-th/0008151].

[8] D. Dominici, B. Grzadkowski, J. F. Gunion and M. Toharia, "The Scalar sector of the Randall-Sundrum model," Nucl. Phys. B **671**, 243 (2003) [hep-ph/0206192].

[9] N. Desai, U. Maitra and B. Mukhopadhyaya, "An updated analysis of radion-higgs mixing in the light of LHC data," arXiv:1307.3765.

[10] M. Battaglia, S. De Curtis, A. De Roeck, D. Dominici and J. F. Gunion, "On the complementarity of Higgs and radion searches at LHC," Phys. Lett. B **568**, 92 (2003) [hep-ph/0304245].

[11] K. Cheung, C. S. Kim and J. -h. Song, "A Probe of the radion Higgs mixing in the Randall-Sundrum model at e+ e- colliders," Phys. Rev. D **67**, 075017 (2003) [hep-ph/0301002].

[12] G. Abbiendi *et al.* [OPAL Collaboration], "Search for radions at LEP2," Phys. Lett. B **609**, 20 (2005) [Erratum-ibid. B **637**, 374 (2006)] [hep-ex/0410035].

[13] S. Bae, P. Ko, H. S. Lee and J. Lee, "Radion phenomenology in the Randall-Sundrum scenario," hep-ph/0103187 and S. Bae, P. Ko, H. S. Lee and J. Lee, "Phenomenology of the radion in Randall-Sundrum scenario at colliders," Phys. Lett. B **487**, 299 (2000) [hep-ph/0002224].

[14] U. Mahanta and A. Datta, "Production of light stabilized radion at high-energy hadron collider," Phys. Lett. B **483**, 196 (2000) [hep-ph/0002183].

[15] G. Aad *et al.* [ATLAS Collaboration], "Observation of a new particle in the search for the Standard Model Higgs boson with the ATLAS detector at the LHC," Phys. Lett. B **716**, 1 (2012) [arXiv:1207.7214 [hep-ex]].

[16] S. Chatrchyan *et al.* [CMS Collaboration], "Observation of a new boson at a mass of 125 GeV with the CMS experiment at the LHC," Phys. Lett. B **716**, 30 (2012) [arXiv:1207.7235 [hep-ex]].

[17] G. -C. Cho, D. Nomura and Y. Ohno, "Constraints on radion in a warped extra dimension model from Higgs boson searches at the LHC," Mod. Phys. Lett. A **28**, 1350148 (2013) [arXiv:1305.4431 [hep-ph]].

[18] J. F. Gunion, M. Toharia and J. D. Wells, "Precision electroweak data and the mixed Radion-Higgs sector of warped extra dimensions," Phys. Lett. B **585**, 295 (2004) [hep-ph/0311219].

[19] V. Barger and M. Ishida, "Randall-Sundrum Reality at the LHC," Phys. Lett. B **709**, 185 (2012) [arXiv:1110.6452 [hep-ph]].

[20] C. Adolphsen, M. Barone, B. Barish, K. Buesser, P. Burrows, J. Carwardine, J. Clark and Hln. M. Durand *et al.*, "The International Linear Collider Technical Design Report - Volume 3.II: Accelerator Baseline Design," arXiv:1306.6328 [physics.acc-ph].

[21] J. F. Gunion, "The Need for a photon-photon collider in addition to LHC & ILC for unraveling the scalar sector of the Randall-Sundrum model," hep-ph/0410379.

[22] M. Chaichian, K. Huitu, A. Kobakhidze and Z. H. Yu, "Radions in a gamma gamma collider," Phys. Lett. B **515**, 65 (2001) [hep-ph/0106077].

[23] K. -m. Cheung, "Phenomenology of radion in Randall-Sundrum scenario," Phys. Rev. D **63**, 056007 (2001) [hep-ph/0009232].

[24] S. Fichet, G. von Gersdorff, O. Kepka, B. Lenzi, C. Royon and M. Saimpert, "Probing new physics in diphoton production with proton tagging at the Large Hadron Collider," arXiv:1312.5153 [hep-ph].

[25] C. Csaki, M. Graesser, L. Randall and J. Terning, "Cosmology of brane models with radion stabilization," Phys. Rev. D **62**, 045015 (2000) [hep-ph/9911406].

[26] K. -m. Cheung, "Associated production of intermediate Higgs or Z boson with $t\bar{t}$ pair in $\gamma\gamma$ collisions," Phys. Rev. D **47**, 3750 (1993) [hep-ph/9211262].

[27] V. I. Telnov, "Physics goals and parameters of photon colliders," Int. J. Mod. Phys. A **13**, 2399 (1998) [hep-ex/9802003].

[28] A. Djouadi, "The Anatomy of electro-weak symmetry breaking. I: The Higgs boson in the standard model," Phys. Rept. **457**, 1 (2008) [hep-ph/0503172].

[29] B. Badelek *et al.* [ECFA/DESY Photon Collider Working Group Collaboration], "TESLA: The Superconducting electron positron linear collider with an integrated X-ray laser laboratory. Technical design report. Part 6. Appendices. Chapter 1. Photon collider at TESLA," Int. J. Mod. Phys. A **19**, 5097 (2004) [hep-ex/0108012].

[30] T. Behnke, J. E. Brau, B. Foster, J. Fuster, M. Harrison, J. M. Paterson, M. Peskin and M. Stanitzki *et al.*, "The International Linear Collider Technical Design Report - Volume 1: Executive Summary," arXiv:1306.6327 [physics.acc-ph].

[31] T. Behnke, J. E. Brau, P. N. Burrows, J. Fuster, M. Peskin, M. Stanitzki, Y. Sugimoto and S. Yamada *et al.*, "The International Linear Collider Technical Design Report - Volume 4: Detectors," arXiv:1306.6329 [physics.ins-det].

[32] CMS collaboration, "Properties of the Higgs-like boson in the decay $H \to ZZ \to 4\ell$ in pp collisions at $\sqrt{s} = 7$ and 8 TeV", CMS PAS HIG-13-002 (2013).

[33] CMS collaboration, "Update on the search for the standard model Higgs boson in pp collisions at the LHC decaying to W^+W^- in the fully leptonic final state", CMS PAS HIG-13-003 (2013).

[34] CMS collaboration, "Updated measurements of the Higgs boson at 125 GeV in the two photon decay channel", CMS PAS HIG-13-001 (2013).

[35] Y. Ohno, in progress.